

A Wideband Frequency Tunable Optoelectronic Oscillator Incorporating a Tunable Microwave Photonic Filter Based on Phase-Modulation to Intensity-Modulation Conversion Using a Phase-Shifted Fiber Bragg Grating

Wangzhe Li, *Student Member, IEEE*, and Jianping Yao, *Fellow, IEEE*

Abstract—An optically tunable optoelectronic oscillator (OEO) with a wide frequency tunable range incorporating a tunable microwave photonic filter implemented based on phase-modulation to intensity-modulation conversion using a phase-shifted fiber Bragg grating (PS-FBG) is proposed and experimentally demonstrated. The PS-FBG in conjunction with two optical phase modulators in the OEO loop form a high-Q, wideband and frequency-tunable microwave photonic bandpass filter, to achieve simultaneously single-frequency selection and frequency tuning. Since the tuning of the microwave filter is achieved by tuning the wavelength of the incident light wave, the tunability can be easily realized at a high speed. A theoretical analysis is performed, which is verified by an experiment. A microwave signal with a frequency tunable from 3 GHz to 28 GHz is generated. To the best of our knowledge, this is the widest frequency tunable range ever achieved by an OEO. The phase noise performance of the OEO is also investigated.

Index Terms—Microwave generation, microwave photonics, optoelectronic oscillator (OEO), phase modulation, phase-shifted fiber Bragg grating.

I. INTRODUCTION

MICROWAVE signal generation using an optoelectronic oscillator (OEO) [1]–[3] has been considered a promising solution for the generation of a high frequency and ultra-low phase noise microwave signal, and it can find important applications in optical and wireless communications, radar, modern instrumentation, microwave imaging and microwave spectroscopy [4]. To reduce the phase noise, a simple solution is to design an OEO to have a long fiber loop, but an OEO with a long loop length will have a large number of densely-spaced oscillation modes. To ensure that the OEO operates at a single oscillation mode, a high-Q electrical bandpass filter (BPF) is

required. To ease the requirement for a high-Q BPF, the use of multiple loops in an OEO, to make the mode spacing greater, has been proposed [5]–[7]. However, the system would become complicated and the stability would deteriorate due to the multiple loop nature of the configuration. In addition, the use of an electrical BPF has some limitations. First, an electrical BPF usually has a fixed central frequency and the implementation of frequency-tunable electrical BPFs is difficult. Thus, an OEO using an electrical BPF can only generate a microwave signal with a small frequency tunable range, realized by slightly changing the mode spacing of the OEO. For example, in [8], [9], the change of the mode spacing of an OEO is achieved via changing the loop delay by employing a dispersive optical fiber loop and a slow light element. The frequency tunable range can be several or tens of MHz, limited by the narrow bandwidth of the electrical BPF in the loop. Second, the central frequency of an electrical BPF with a 3-dB bandwidth of a few MHz is usually low; therefore, the frequency of the generated microwave signal is also low. To solve these problems, we have recently proposed two techniques [10], [11]. In [10], a Fabry–Perot laser diode (FP-LD) is employed to serve as a tunable high-Q microwave photonic BPF. Due to the external injection, the FP-LD selectively amplifies one of the modes, and high frequency selection is ensured. The frequency tuning is realized by either changing the wavelength of the incident light wave or the longitudinal modes of the FP-LD. The major limitation of the technique is the mode hopping in the FP-LD, which may deteriorate the quality of the generated microwave signal. In [11], a high-Q photonic microwave BPF is formed by a phase modulator (PM) followed by a linearly chirped fiber Bragg grating. The frequency tuning is realized by tuning the dispersion of the linearly chirped fiber Bragg grating [12]. To ensure a large frequency tunable range, the dispersion must be tuned in a large range, which is hard to realize for a practical system.

In this paper, a novel approach to realizing a wideband and frequency tunable OEO using a microwave photonic filter is proposed and experimentally demonstrated. The microwave photonic filter has a high Q and a large frequency tunable range, which is implemented using two cascaded PMs and a phase-shifted fiber Bragg grating (PS-FBG). By tuning the

Manuscript received September 28, 2011; revised February 15, 2012; accepted February 21, 2012. Date of publication March 14, 2012; date of current version May 25, 2012. This work was supported by the Natural Sciences and Engineering Research Council of Canada (NSERC).

The authors are with the Microwave Photonics Research Laboratory, School of Electrical Engineering and Computer Science, University of Ottawa, Ottawa, ON K1N 6N5, Canada (e-mail: jpyao@ecees.uottawa.ca).

Color versions of one or more of the figures in this paper are available online at <http://ieeexplore.ieee.org>.

Digital Object Identifier 10.1109/TMTT.2012.2189231

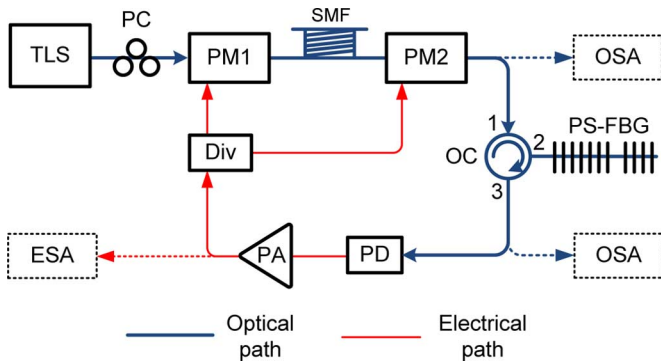


Fig. 1. Schematic of the proposed wideband frequency-tunable OEO.

wavelength of the laser source, the central frequency of the high-Q microwave photonic BPF is tuned. The key significance of the proposed approach is that no electrical filters are employed, which ensures a simple tuning and a large frequency tunable range. In addition, the PMs are not dc biased, which would eliminate the bias drifting problem existing in a Mach-Zehnder modulator (MZM). A theoretical analysis is performed, which is validated by an experiment. The generation of a microwave signal tunable from 3 GHz to 28 GHz is demonstrated. To the best of our knowledge, this is the widest frequency tunable range ever achieved using an OEO. The phase noise performance of the generated microwave signal is also investigated. A modified Yao-Maleki model [2] is also presented to study the phase noise performance, which is also verified by the experiment.

II. PRINCIPLE OF OPERATION

The implementation of the wideband and frequency tunable OEO incorporating a tunable microwave photonic BPF based on phase-modulation to intensity-modulation conversion using a PS-FBG is discussed in this section. Fig. 1 shows a schematic of the proposed frequency-tunable OEO. The OEO consists of a tunable laser source (TLS), two PMs, a single-mode fiber (SMF) connecting the two PMs, an optical circulator (OC), a PS-FBG with a phase shift of π , a photodetector (PD), a microwave power amplifier (PA), and a microwave power divider (Div). A light wave from the TLS is sent to the two cascaded PMs (PM1 and PM2) connected by the SMF. The phase-modulated light wave is sent to the PS-FBG via the OC, reflected by the PS-FBG and sent to the PD via again the OC. The signals at the output of PM2 and at the input of the PD are monitored by two optical spectrum analyzers (OSAs). After electrical amplification by the PA, the signal at the output of the PD is split into two parts by the power divider, and applied to the two PMs via the RF ports. The signal at the output of the PD is also monitored by an electrical spectrum analyzer (ESA, Agilent E4448A).

To understand the operation and the frequency tuning of the OEO, we start our discussion from the equivalent wideband frequency-tunable microwave photonic BPF that is incorporated in the OEO loop. Such a microwave photonic BPF is based on phase modulation using the PM and phase-modulation to intensity-modulation conversion using the PS-FBG. The schematic of the equivalent microwave photonic BPF is shown in Fig. 2. Its frequency response is measured by a vector network ana-

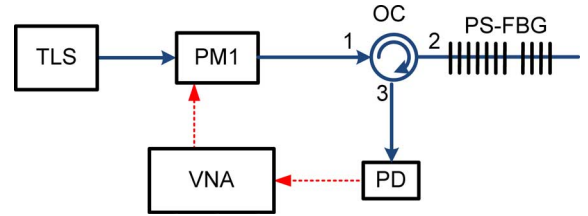


Fig. 2. Schematic of the equivalent wideband frequency-tunable microwave photonic BPF.

lyzer (VNA). The VNA generates a microwave signal with its frequency sweeping over a frequency range of interest, and the received microwave signal at the output of the PD is sent back to the VNA.

We assume that PM1 is driven by a microwave signal given by $V_e \cos \Omega t$, where V_e is the amplitude and Ω is the angular frequency of the microwave signal. The electrical field $E_{PM1}(t)$ at the output of PM1, under the small-signal modulation condition, can be expressed as

$$\begin{aligned} E_{PM1}(t) &= E_0 \exp \left\{ j \left[\omega_o t + \pi \frac{V_e}{V_\pi} \cos(\Omega t) \right] \right\} \\ &\approx E_0 \{ J_0(\beta) \exp(j\omega_o t) \\ &\quad + J_1(\beta) \exp[j(\omega_o t + \Omega t + \pi/2)] \\ &\quad - J_1(\beta) \exp[j(\omega_o t - \Omega t - \pi/2)] \} \end{aligned} \quad (1)$$

where E_0 is the unit amplitude of the electrical field of the incident light wave, ω_o is the angular frequency of the incident light wave, V_π is the half-wave voltage of the drive signal, J_0 and J_1 are the 0th- and 1st-order Bessel functions of the first kind, $\beta = \pi V_e / V_\pi$ is the phase modulation index. When β is small, say less than 0.5, the powers of the higher order sidebands (the order of the Bessel function is equal to or larger than 2) are much less than those of the first-order sidebands and the optical carrier. Therefore, these higher order sidebands are ignored.

As can be seen, the signal at the output of PM1 contains an optical carrier and two 1st-order sidebands. If the light wave is directly applied to the PD, no signal would be detected except a dc since the beating between the optical carrier and the upper sideband will cancel completely the beating between the optical carrier and the lower sideband, due to the fact that the two beat signals are out of phase. However, if the amplitude and/or the phase profile of the phase-modulated light wave in its frequency domain is changed, the phase-modulated light wave can be converted to an intensity-modulated light wave, and phase-modulation to intensity-modulation conversion has a transfer function corresponding to a microwave photonic BPF [13]. To achieve a narrow passband, the change of the profile should only occur over a small frequency range. Thus, a PS-FBG is an ideal device since a PS-FBG could have an ultra-narrow notch with fast phase variations in the reflection spectrum [14], and the use of the PS-FBG could modify the amplitude and the phase of one of the two 1st-order sidebands of the phase-modulated light wave within an ultra-narrow bandwidth. The operation is illustrated in Fig. 3.

The ultra-narrow passband only appears when one sideband falls into the notch of the PS-FBG, and the central frequency

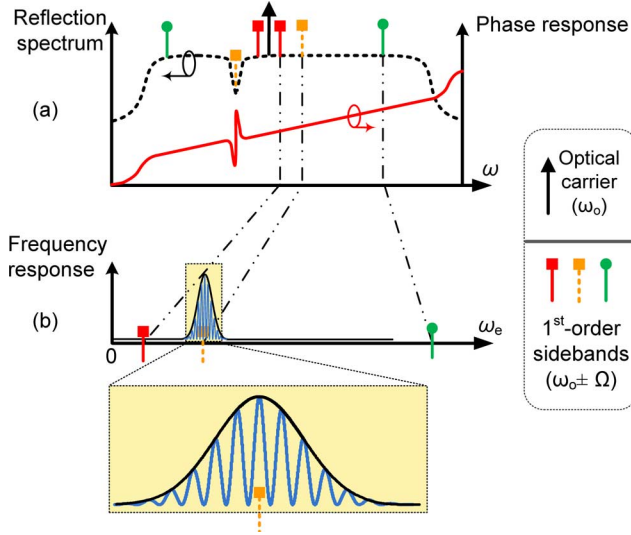


Fig. 3. The equivalent high-Q microwave photonic BPF. (a) The reflection spectrum and phase response profile of the PS-FBG; (b) The frequency response of the photonic microwave BPF.

of the passband is equal to the frequency spacing between the notch and the incident light wave. Since the notch of the PS-FBG can be controlled as narrow as a few MHz [15], accordingly the bandwidth of the microwave photonic BPF can be as narrow as a few MHz, thus a microwave photonic BPF with a high-Q factor is achieved. The tunability of the microwave photonic BPF can be easily realized by simply tuning the wavelength of the light wave from the TLS. Another important feature of the microwave photonic BPF is the large frequency tunable range. As can be seen from Fig. 3, the largest tunable range is limited by the reflection bandwidth of the PS-FBG, and the bandwidth of the PM, the PD and the PA. Since the bandwidths of the PDs, PAs and PMs as well as the reflection bandwidth of the PS-FBG can be tens of GHz and are commercially available now, the frequency tuning range of the microwave photonic BPF could be also as large as tens of GHz. Therefore, due to the incorporation of the microwave photonic BPF in the OEO loop, a microwave signal with an oscillation frequency that is tunable over a frequency range of tens of GHz can be generated.

The bandwidth of the microwave photonic BPF can be further reduced if a second PM is employed. As can be seen from Fig. 1, the two PMs are connected by a length of SMF. If PM2 is connected to PM1 through the SMF, then the phase-modulated light wave is given by

$$\begin{aligned}
 E_{PM2}(t) &= E_0 \\
 &\times \exp \left\{ j \left[\omega_o t + \pi \frac{V_e}{V_\pi} \cos(\Omega t) + \pi \frac{V_e}{V_\pi} \cos[\Omega(t + \tau)] \right] \right\} \\
 &= E_0 \exp \{ j[\omega_o t + \beta'(\Omega) \cdot \cos[\Omega t + \Omega\tau/2]] \} \\
 &\approx E_0 \{ J_0[\beta'(\Omega)] \exp(j\omega_o t) \\
 &+ J_1[\beta'(\Omega)] \exp[j(\omega_o t + \Omega t + \Omega\tau/2 + \pi/2)] \\
 &- J_1[\beta'(\Omega)] \exp[j(\omega_o t - \Omega t - \Omega\tau/2 - \pi/2)] \} \quad (2)
 \end{aligned}$$

where $\tau = Ln_o/c$ is the time delay introduced by the SMF, where L is the length of the SMF, c is the velocity of light in vacuum, n_o is the refractive index of the SMF, and $\beta'(\Omega) = 2\pi V_e \cos(\Omega\tau/2)/V_\pi$ is an equivalent phase modulation index, which is not a constant but a sinusoidal function of Ω . Consequently, phase-modulation to intensity-modulation conversion would have a transfer function that is equal to the product of the frequency response of the ultra-narrow microwave photonic BPF and the frequency response of the sinusoidal comb filter, as shown in the zoom-in view of Fig. 3(b). The transmission peaks of the comb filter are located at the frequencies when $|\beta'(\Omega)| = 2\pi V_e/V_\pi$, namely, $\Omega = 2\pi k/\tau$, where k is an integer. The distance between two adjacent peaks is $2\pi c/Ln_o$.

After reflection by the PS-FBG, the electrical field $E_{IM}(t)$ of the light wave at the input of the PD can be expressed as

$$\begin{aligned}
 E_{IM}(t) &\approx E_0 J_0[\beta'(\Omega)] \exp(j\omega_o t + j\omega_o \tau') \\
 &+ E_0 J_1[\beta'(\Omega)] \\
 &\times \exp[j(\omega_o t + \Omega t + \Omega\tau/2 \\
 &+ \pi/2 + \omega_o \tau' + \Omega\tau')] \\
 &- E_0 r(\omega_o - \Omega) \cdot J_1[\beta'(\Omega)] \\
 &\times \exp[j(\omega_o t - \Omega t - \Omega\tau/2 - \pi/2 \\
 &+ \omega_o \tau' - \Omega\tau')] \quad (3)
 \end{aligned}$$

where $r(\omega)$ is the reflection profile of the PS-FBG, where ω is the angular frequency of the light wave incident to the PS-FBG, $\tau' = L'n_o/c$ is the time delay introduced by the short fiber between PM2 and the PD, where L' is the length of the short fiber. Then, the microwave signal at the output of the PD can be expressed as

$$\begin{aligned}
 V(\Omega, t) &\propto R |E_{IM}(t)|^2 \\
 &= R [1 - r(\omega_o - \Omega)] J_0[\beta'(\Omega)] J_1[\beta'(\Omega)] \\
 &\times \sin[\Omega t + \Omega\tau + \Omega\tau'] \\
 &\approx R [1 - r(\omega_o - \Omega)] \pi V_e/V_\pi \cos(\Omega\tau/2) \\
 &\times \sin[\Omega t + \Omega\tau + \Omega\tau'] \quad (4)
 \end{aligned}$$

where R is the photo-responsivity of the PD, $J_0[\beta'(\Omega)] \approx 1$ and $J_1[\beta'(\Omega)] \approx \beta'(\Omega)/2$ when $\beta'(\Omega)$ is small, say less than 0.5. Therefore, the frequency response $H(\Omega)$ can be given by

$$H(\Omega) = \frac{V(\Omega)^2}{V_e^2} \approx \frac{\pi^2 R^2}{V_\pi^2} \cdot [1 - r(\omega_o - \Omega)]^2 \cdot \left[\frac{1 + \cos(\Omega\tau)}{2} \right]. \quad (5)$$

In (5), the term $[1 - r(\omega_o - \Omega)]^2$ represents the frequency response when only a single PM is used. The peak of the pass band appears when $r(\omega_o - \Omega) = 0$, which means that the lower sideband is completely suppressed. The other term, $[1 + \cos(\Omega\tau)]/2$, is the frequency response of the comb filter.

If the gain in the loop is greater than the loss, once the loop is closed, the OEO will start to oscillate. The total output at the

PD at any instant time is the summation of all circulating fields in the loop, which can be expressed as

$$\begin{aligned}
 V'(\Omega, t) &= \exp(j\Omega t) \times \sum_{m=0}^{\infty} \{RG(1-r)\pi V_e/V_\pi \cos(\Omega\tau/2)\}^m \\
 &\quad \cdot \exp(jm\Omega\tau + jm\Omega\tau') \\
 &= \exp(j\Omega t) \times \sum_{m=0}^{\infty} [G_{\text{eff}}(\Omega)]^m \cdot \exp(jm\Omega\tau + jm\Omega\tau')
 \end{aligned} \tag{6}$$

where G is the voltage gain provided by the PA, m is the number of times the light wave circulates in the loop, and $G_{\text{eff}}(\Omega)$ is the effective open-loop gain, given by

$$G_{\text{eff}}(\Omega) = RG(1-r)\pi V_e/V_\pi \cos(\Omega\tau/2). \tag{7}$$

After the OEO starts oscillation, the effective open-loop gain G_{eff} is a little less than unity, (6) can then be simplified to

$$V'(\Omega, t) = \frac{\exp(j\Omega t)}{1 - G_{\text{eff}}(\Omega) \cdot \exp(j\Omega\tau + j\Omega\tau')}. \tag{8}$$

The corresponding microwave power $P(\omega_e, t)$ is then given

$$\begin{aligned}
 P(\Omega, t) &\propto |V'(\Omega, t)|^2 \\
 &= \frac{1}{1 + G_{\text{eff}}^2(\Omega) - 2G_{\text{eff}}(\Omega) \cdot \cos(\Omega\tau + \Omega\tau')}.
 \end{aligned} \tag{9}$$

Only when the two phase delays $\Omega\tau$ and $\Omega\tau'$ are multiples of 2π after each loop circulation, and $r(\omega_o - \Omega) = 0$, $|G_{\text{eff}}(\Omega)|$ would reach a maximum value, and the corresponding frequency will oscillate. At an oscillation frequency Ω_{osc} , (9) can be rewritten as

$$P(\Omega_{\text{osc}}, t) \propto \frac{1}{[1 - RG\pi V_e/V_\pi]^2}. \tag{10}$$

Then, when the wavelength of the TLS, ω_o , is tuned to make $r(\omega_o - \Omega) = 0$, ω_e will automatically change to Ω' in the same direction of ω_o . If both $\Omega'\tau$ and $\Omega'\tau'$ are multiples of 2π , Ω' will be a new oscillation frequency, and frequency tuning is thus achieved.

III. EXPERIMENT AND DISCUSSION

An experiment based on the setup shown in Fig. 1 is performed (see Fig. 4). The TLS (Yokogawa AQ 2200-136) has a wavelength tunable range of 200 nm and a tuning step of 1 pm. The bandwidths of the PMs are 20 GHz. The PA in Fig. 1 consists of one Avanteck low-noise amplifier and an Agilent 83006A amplifier. The PD (Newport) has a bandwidth of 45 GHz. The PCs are used to minimize the polarization-dependent loss. The key device in the system is the PS-FBG, which is fabricated in a photosensitive fiber using a uniform phase mask by scanning an UV beam along the axial direction of the optical fiber [15]. A π phase shift is introduced at the center of the grating by shifting the phase mask by half the corrugation

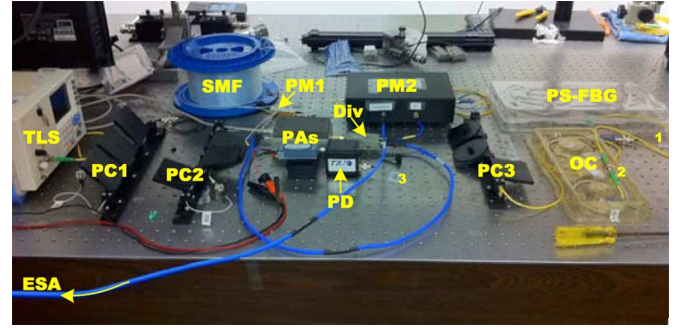


Fig. 4. Photograph of the experimental setup. Numbers 1, 2 and 3 in the photograph indicate port 1, port 2, and port 3 of the OC.

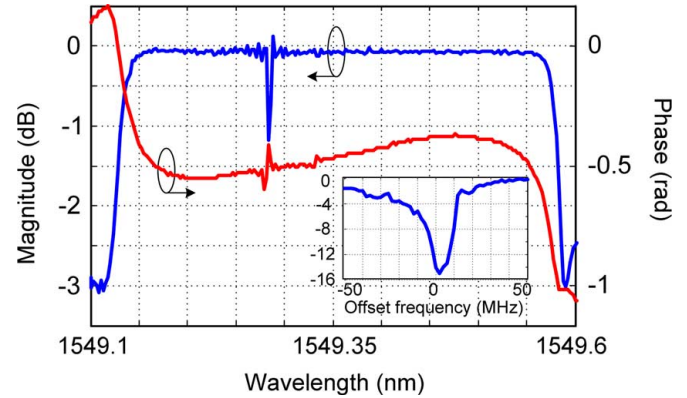


Fig. 5. Measured reflection magnitude response and phase response of the PS-FBG (resolution: 0.01 nm). The inset gives a zoom-in view of the notch of the PS-FBG (resolution: 2 MHz).

width to create an ultra-narrow notch at the middle of the reflection spectrum. The PS-FBG is fabricated by introducing a phase shift during the fabrication process. An ultra-narrow transmission band in the reflection spectrum is thus generated. The measured reflection magnitude response and phase response of the PS-FBG are shown in Fig. 5. The 3-dB reflection bandwidth is about 0.5 nm. The centre wavelength of the notch is about 1549.28 nm, with a full-width at half-maximum (FWHM) of only about 30 MHz. The maximum notch depth is more than 15 dB.

First of all, the frequency response of the equivalent wide-band frequency-tunable photonic microwave BPF based on phase-modulation to intensity-modulation conversion is measured. To do so, the loop is opened at the output port of the PD, and only one PM is used. The frequency response is measured using a VNA (Agilent E8364A). The powers of the light wave sent to the PM and to the PD are measured to be about 5 dBm and 0 dBm, respectively. The wavelength of the optical carrier is set around 1549.28 nm, and the lower sideband will fall into the notch of the PS-FBG when the microwave frequency is equal to the difference between the frequency of the optical carrier and the center frequency of the notch. By increasing the wavelength of the optical carrier, the center frequency of the photonic microwave BPF is increased. Fig. 6(a) shows the superimposed frequency responses of the microwave photonic BPF with a tunable central frequency covering a range of about

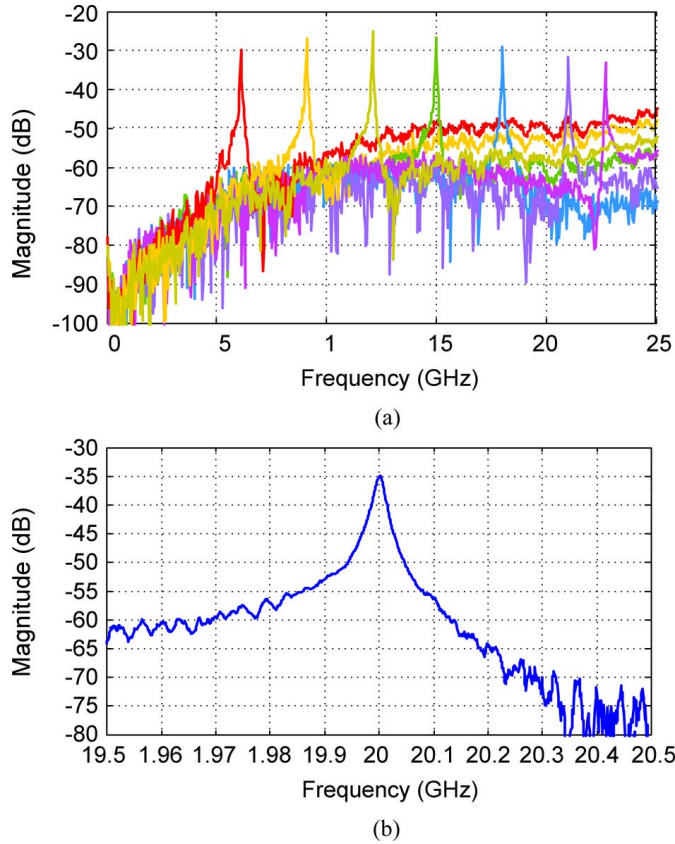


Fig. 6. (a) Measured frequency responses of the tunable photonic microwave BPF. (b) Zoom-in view of the frequency response when the center frequency is tuned at 20 GHz.

20 GHz. This range can be increased if the reflection bandwidth of the PS-FBG is wider. From Fig. 6(a) we can see that the ratio of the transmission peak to the sidelobe can be as large as 30 dB, which is large enough to suppress undesired modes in the OEO. In Fig. 6(b), a zoom-in view of the measured frequency response with a central frequency of 20 GHz is shown. The 3-dB bandwidth is about 20 MHz, corresponding to a Q -factor of 1000. If the index change of the grating is increased or the degree of the symmetry of the two sub-gratings separated by the phase shift section is improved, the PS-FBG would have a narrower notch and the 3-dB bandwidth of the microwave photonic filter can be further decreased.

Then, the OEO loop is closed. The length of the SMF is about 500 m, corresponding to a time delay τ of about 2.43 μ s. The length between PM2 and the power divider is about 10 m, corresponding to a time delay τ' of about 48.6 nm. The wavelength of the light wave is first set at 1549.36 nm, which is about 0.08 nm away from the central wavelength of the transmission band; thus Ω would be approximately equal to 10 GHz. By finely tuning the wavelength of the light wave to make $\Omega\tau$ and $\Omega\tau'$ are multiples of 2π , the OEO will start oscillation at 10 GHz. At the oscillation frequency, the phase modulation indexes of PM1 and PM2 are about 0.25, giving an equivalent phase modulation index, $\beta'(\Omega_{osc})$, of 0.5. Fig. 7 shows the measured optical spectrum at the outputs of PM2 and the PS-FBG. As expected, after reflection from the PS-FBG the power of the lower sideband of the phase-modulated light wave is attenuated, which is 10 dB lower

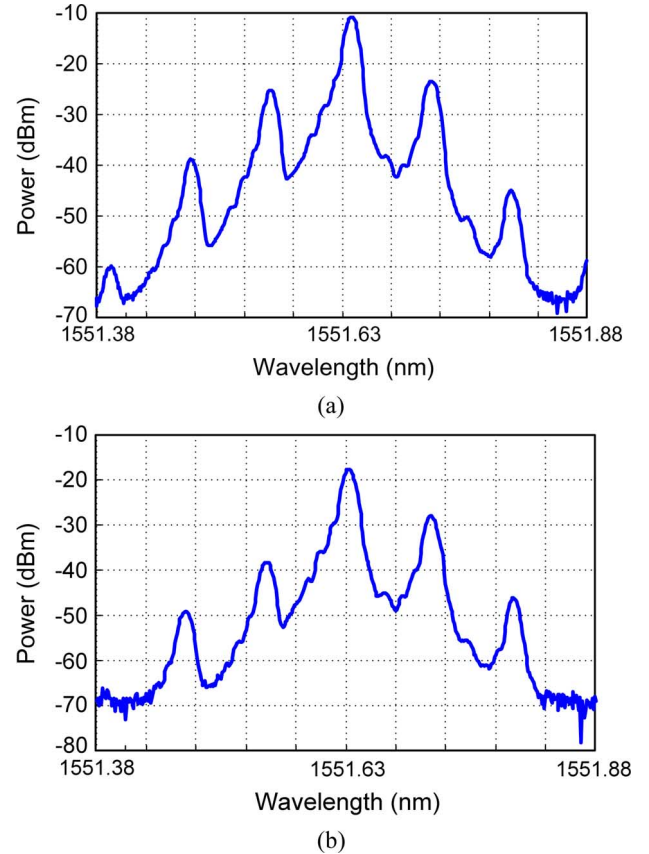


Fig. 7. (a) Optical spectrum at the output of PM2 when the OEO is operated at 10 GHz. (b) Optical spectrum at the output of the PS-FBG when the OEO is operated at 10 GHz.

than that of the upper sideband. Although the lower sideband is not completely removed, the residual power is very small, and an effective phase-modulation to intensity-modulation conversion is achieved. Fig. 8 shows the spectrum of the generated 10-GHz signal with two different frequency spans of 25 GHz and 200 KHz. No other modes are observed.

The stability of the system is evaluated. To do so, the system is allowed to operate in a room environment for a period of 10 minutes. The spectrum of the 10-GHz signal is shown on the ESA with negligible power fluctuations. The frequency stability is also evaluated. Due to the wavelength drift of the TLS and the spectrum drift of the unpackaged PS-FBG, a frequency shift of a few MHz is observed after an hour. The use of a wavelength-stabilized laser source and a packaged PS-FBG would increase significantly the frequency stability.

The frequency tunability of the proposed OEO is then investigated. Both coarse tuning and fine tuning are demonstrated. The tuning is realized by tuning the wavelength of the TLS. The smallest wavelength tuning step of the TLS is 1 pm, corresponding to a frequency tuning step of about 125 MHz. Fig. 9(a) shows the superimposed spectra of the generated microwave signal with the frequency coarsely tuned over a frequency range from 3 GHz to 14 GHz with a tuning step of 1 GHz. Fig. 9(b) shows the superimposed spectra of the generated microwave signal with the frequency coarsely tuned over a frequency range from 15 GHz to 28 GHz with a tuning step of 1 GHz. Thus,

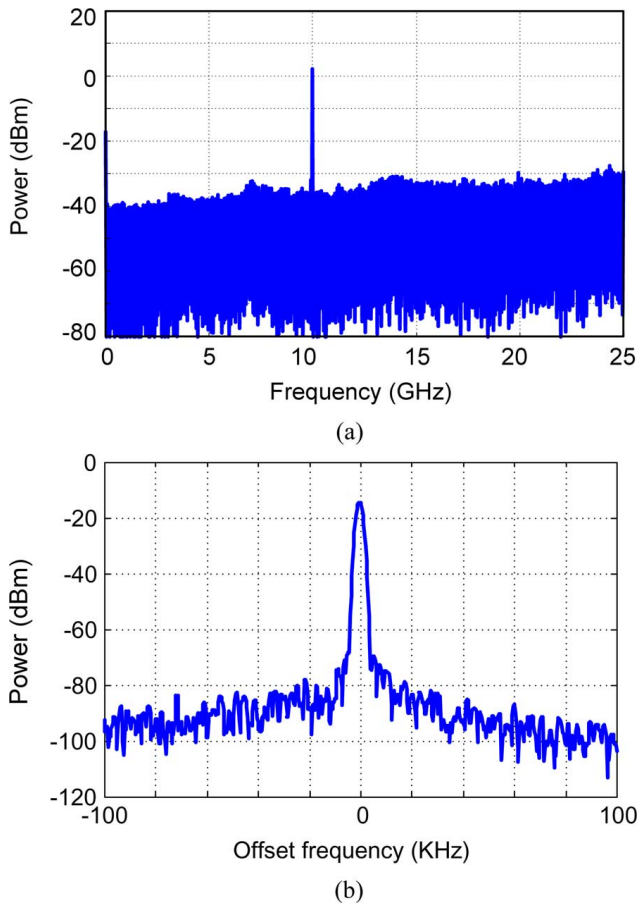


Fig. 8. Generation of a 10-GHz microwave signal using the proposed OEO. (a) Electrical spectrum of the generated 10-GHz signal (the frequency span is 30 GHz and the resolution bandwidth (RBW) is 3 MHz). (b) Zoom-in view of the 10-GHz signal (the frequency span is 200 KHz and the RBW is 1.8 KHz).

the total frequency tuning range of the proposed OEO is about 25 GHz. Fig. 9(c) shows the superimposed spectra with the frequency finely tuned from about 9.2 GHz to about 10.7 GHz with a tuning step of about 125 MHz. The tuning step can be smaller, but it is limited here by the wavelength tuning resolution of the TLS, which is 1 pm.

The main factor limiting the tunable range of the OEO is the limited reflection bandwidth of the PS-FBG. It is known that a wider reflection bandwidth can be achieved if the amplitude of the induced refractive index perturbation Δn is larger [16]. To achieve a large Δn , the fiber could be hydrogen loaded and the grating could be written by using IR femtosecond pulses [17], which potentially give a reflection bandwidth as large as a few nanometers. For example, if the reflection bandwidth of the PS-FBG is 2.4 nm, then the frequency tunable range of the microwave photonic filter can be 100 GHz [18], which also gives a frequency tunable range of the OEO of 100 GHz. If the PS-FBG is fabricated in a silicon-on-insulator waveguide by using deep-ultraviolet lithography, an even wider reflection bandwidth as large as 10 nm can be achieved [19], which could give a tunable range as large as hundreds of GHz.

The phase noise performance of the generated microwave signals is also studied. The analysis is done by modifying the

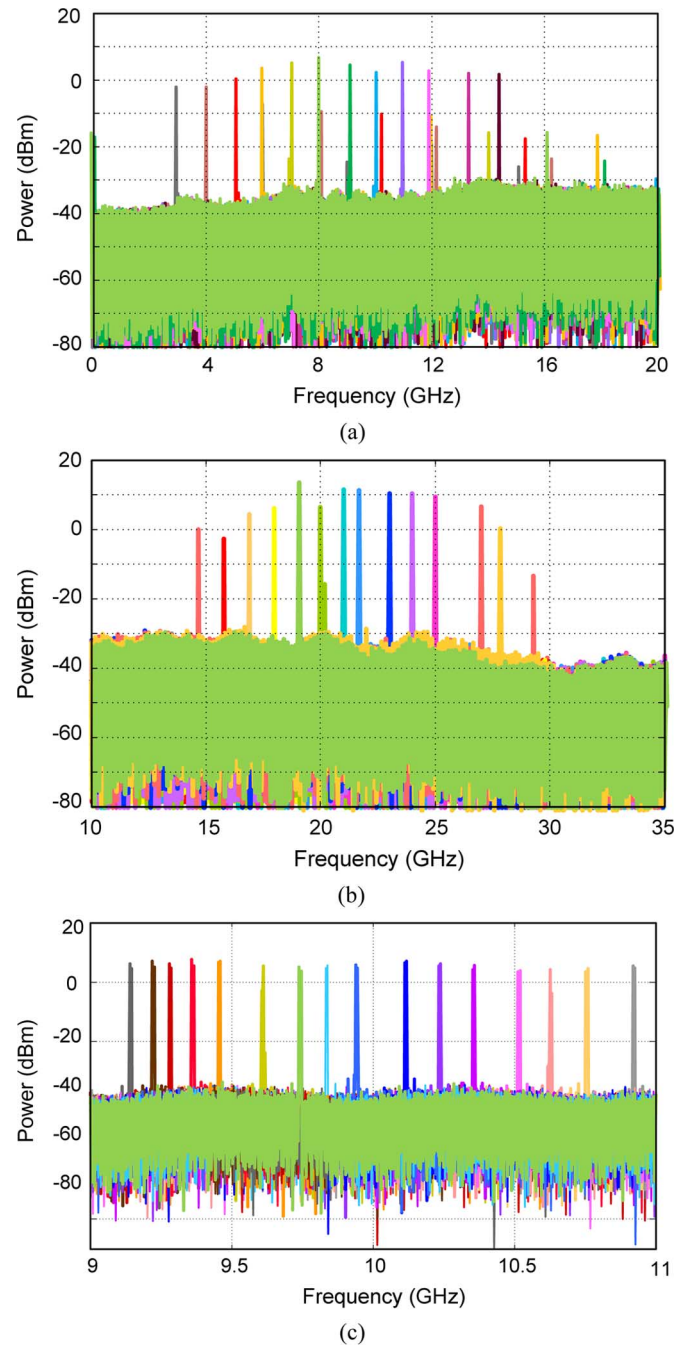


Fig. 9. Spectra of the generated microwave signal at different frequencies. (a) The frequency is coarsely tuned from 3 GHz to 14 GHz with a tuning step of 1 GHz; the RBW is 10 MHz. (b) The frequency is coarsely tuned from 15 GHz to 28 GHz with a tuning step of 1 GHz; the RBW is 3 MHz. (c) The frequency is finely tuned from 9.2 GHz to 10.8 GHz with a tuning step of about 125 MHz; the RBW is 3 MHz.

Yao-Maleki equation which was developed to characterize the phase noise power spectral density of an OEO. The modified equation gives a phase noise power spectral density with a better agreement with the experimental results. The Yao-Maleki equation is given by [2]

$$S(f') = \frac{\delta}{(\delta/2\tau)^2 + (2\pi)^2(\tau f')^2} \quad (11)$$

where f' is the frequency offset from the oscillation frequency, and δ is the input noise-to-signal ratio to the OEO, given by

$$\delta = \rho_N G_A^2 / P_{\text{osc}} \quad (12)$$

where ρ_N is the equivalent input noise power density injected into the OEO from the input port of the PA, which has a typical value of 10^{-17} mW/Hz, P_{osc} is the power of the signal at the oscillation frequency applied to the PMs, and G_A is the voltage gain of the PA. Thus, P_{osc}/G_A^2 is the power of the oscillation frequency before the PA, which has a typical value of 10^{-4} mW. Therefore, δ has a typical value of 10^{-13} /Hz.

Based on (11) and (12), we calculated the theoretical single-sideband phase noise spectrum of the generated microwave signal and compare it with the single-sideband phase noise spectrum of the experimentally generated 10-GHz microwave signal shown in Fig. 10. The single-sideband phase noise spectrum of the generated signal is measured by an Agilent E5052B signal source analyzer incorporating an Agilent E5053A downconverter. The phase noise spectrum calculated based on the standard Yao-Maleki model is also shown in Fig. 10 as a dotted-dashed line. As can be seen the phase noise performance is overestimated by the standard Yao-Maleki model. The difference is due to the fact that the Yao-Maleki model assumes that the noise in the OEO is a strictly white noise source, and ignores other frequency-dependent noise sources which do exist in a real OEO. In our case, such frequency-dependent noise could be the relative intensity noise (RIN) of the TLS, the laser wavelength fluctuations, the length changing of the SMF, and the spectrum variations of the PS-FBG. Here in our analysis, we simply group all the frequency-dependent noise sources into two categories: the noise whose power density is inversely proportional to f' and the noise whose power density is proportional to f' over only a small offset frequency range. Since all the noise sources are supposed to be independent, the power density of the input noise injected into the OEO can be written as

$$\rho'_N = \rho_N + \rho_{N1}/f' + \rho_{N2} \cdot f' \quad (13)$$

where ρ_{N1} and ρ_{N2} are two parameters of the input noise. The input noise-to-signal ratio to the OEO can also be rewritten as

$$\delta' = \rho'_N G_A^2 / P_{\text{osc}} = \delta + \delta_1/f' + \delta_2 \cdot f' \quad (14)$$

where δ_1 and δ_2 are two parameters of the input noise-to-signal ratio. Thus, the modified power density spectrum $S'(f')$ is given by

$$\begin{aligned} S'(f') &= \frac{\delta'}{(\delta'/2\tau)^2 + (2\pi)^2(\tau f')^2} \\ &= \frac{\delta}{(\delta'/2\tau)^2 + (2\pi)^2(\tau f')^2} \\ &\quad + \frac{\delta_1/f'}{(\delta'/2\tau)^2 + (2\pi)^2(\tau f')^2} \\ &\quad + \frac{\delta_2 \cdot f'}{(\delta'/2\tau)^2 + (2\pi)^2(\tau f')^2} \end{aligned} \quad (15)$$

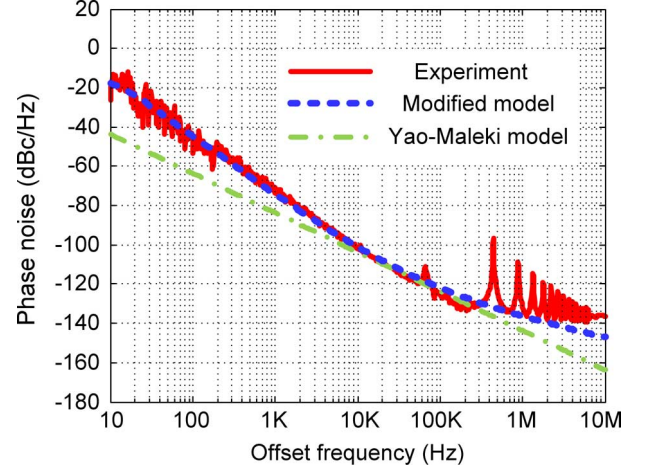


Fig. 10. A comparison of the phase noise based on the Yao-Maleki model, the modified model and experimental data for our proposed OEO.

To fit our experimental data, δ_1 and δ_2 are selected to be 8×10^{-9} and 4.5×10^{-18} /Hz². The calculated phase noise spectrum based on the modified model is shown in Fig. 10 as a dashed line.

From Fig. 10, we can also see that the measured phase noise is -102 dBc/Hz at a 10-KHz offset frequency. The peaks after 400-KHz offset frequency which have a frequency spacing corresponding to a free spectral range of the OEO are resulted from the non-oscillating sidemodes. Another peak at 66-KHz is associated with an uncertain perturbation, and disappears from time to time. The phase noise performance can be further improved by using a wavelength-stabilized TLS and a packaged PS-FBG.

IV. CONCLUSION

A novel approach to implementing a wideband frequency-tunable OEO using a PS-FBG was proposed and experimentally demonstrated. Due to the phase-modulation to intensity-modulation conversion in the PS-FBG, an equivalent high-Q tunable microwave photonic BPF in the OEO loop was established, which was employed to select one of the eigenmodes in the OEO, to achieve single-frequency oscillation. The central frequency of the equivalent microwave photonic BPF could be easily tuned by tuning the wavelength of the TLS, thus leading to the tuning of the frequency of the generated microwave signal. The key significance of the proposed OEO is that it can provide large frequency tunability by simply tuning the optical wavelength. In addition, since no bias control is needed for the PMs, the operation stability is also better than using an MZM. The proposed OEO was verified by an experiment. The generation of a microwave signal with a frequency tunable from 3 GHz to 28 GHz was demonstrated. To the best of our knowledge, this is the widest frequency-tunable range ever achieved by an OEO. The generated microwave signal exhibited a good phase noise performance. A modified Yao-Maleki model was also developed to describe the phase noise performance of the proposed OEO. The phase noise performance of the proposed OEO can be further improved if a packaged PS-FBG and a wavelength-stabilized laser source are employed. The PMs and PS-FBG could be potentially

integrated in a photonic integrated circuit (PIC) chip, which would significantly improve the overall performance of the proposed OEO.

ACKNOWLEDGMENT

The authors would like to thank Dr. M. Poulin for helpful discussions. The authors would also like thank TeraXion, QC, Canada, for providing the PS-FBG.

REFERENCES

- [1] A. Neyer and E. Voges, "Hybrid electro-optical multivibrator operating by finite feedback delay," *Electron. Lett.*, vol. 18, no. 2, pp. 59–60, Jan. 1982.
- [2] X. S. Yao and L. Maleki, "Optoelectronic microwave oscillator," *J. Opt. Soc. Amer. B*, vol. 13, no. 8, pp. 1725–1735, Aug. 1996.
- [3] T. Berceci and P. Herczfeld, "Microwave photonics—A historical perspective," *IEEE Trans. Microw. Theory Tech.*, vol. 58, no. 11, pp. 2992–3000, Nov. 2010.
- [4] X. S. Yao and L. Maleki, "Opto-electronic oscillator and its applications," in *Proc. Microw. Photon. MWP'96, Technical Dig.*, Dec. 1996, pp. 265–268.
- [5] X. S. Yao and L. Maleki, "Multiloop optoelectronic oscillator," *IEEE J. Quantum Electron.*, vol. 36, no. 1, pp. 79–84, Jan. 2000.
- [6] Y. Jiang, J. Yu, Y. Wang, L. Zhang, and E. Yang, "An optical domain combined dual-loop optoelectronic oscillator," *IEEE Photon. Technol. Lett.*, vol. 19, no. 11, pp. 807–809, Jun. 2007.
- [7] E. Shumakher and G. Eisenstein, "A novel multiloop optoelectronic oscillator," *IEEE Photon. Technol. Lett.*, vol. 20, no. 22, pp. 1881–1883, Nov. 2008.
- [8] S. Poinot, H. Porte, J. Goedgebuer, W. T. Rhodes, and B. Boussert, "Continuous radio-frequency tuning of an optoelectronic oscillator with dispersive feedback," *Opt. Lett.*, vol. 27, no. 15, pp. 1300–1302, Aug. 2002.
- [9] E. Shumakher, S. Ó. Dúill, and G. Eisenstein, "Optoelectronic oscillator tunable by an SOA based slow light element," *J. Lightw. Technol.*, vol. 27, no. 18, pp. 4063–4068, Sep. 2009.
- [10] S. Pan and J. P. Yao, "Wideband and frequency-tunable microwave generation using an optoelectronic oscillator incorporating a Fabry–Perot laser diode with external optical injection," *Opt. Lett.*, vol. 35, no. 11, pp. 1911–1913, Jun. 2010.
- [11] W. Li and J. P. Yao, "An optically tunable optoelectronic oscillator," *J. Lightw. Technol.*, vol. 28, no. 18, pp. 2640–2645, Sep. 2010.
- [12] H. Shahoei, M. Li, and J. P. Yao, "Continuously tunable time delay using an optically pumped linearly chirped fiber Bragg grating," *J. Lightw. Technol.*, vol. 29, no. 10, pp. 1465–1472, May 2011.
- [13] F. Zeng and J. P. Yao, "Investigation of phase modulator based all-optical bandpass microwave filter," *J. Lightw. Technol.*, vol. 23, no. 4, pp. 1721–1728, Apr. 2005.
- [14] T. Erdogan, "Fiber grating spectra," *J. Lightw. Technol.*, vol. 15, no. 8, pp. 277–1294, Aug. 1997.
- [15] Y. Painchaud, M. Aubé, G. Brochu, and M. Picard, "Ultra-narrow-band notch filtering with highly resonant fiber Bragg gratings," in *Proc. Bragg Gratings, Photosensitivity, and Poling in Glass Waveguides, OSA Technical Digest (CD)*, 2010, Paper BTuC3.
- [16] P. St. J. Russell, J. L. Archambault, and L. Reekie, "Fiber gratings," *Phys. World*, vol. 6, no. 10, pp. 41–46, Oct. 1993.
- [17] M. Bernier, Y. Sheng, and R. Vallee, "Ultrabroadband fiber Bragg gratings written with a highly chirped phase mask and infrared femtosecond pulses," *Opt. Exp.*, vol. 17, no. 5, pp. 3285–3290, Mar. 2009.
- [18] W. Li, M. Li, and J. P. Yao, "A narrow-passband and frequency-tunable micro-wave photonic filter based on phase-modulation to intensity-modulation conversion using a phase-shifted fiber Bragg grating," *IEEE Trans. Microw. Theory Tech.*, to be published.
- [19] X. Wang, W. Shi, S. Grist, H. Yun, N. A. F. Jaeger, and L. Chrostowski, "Narrow-band transmission filter using phase-shifted Bragg gratings in SOI waveguide," in *Proc. 2011 IEEE Photonics Conf. (PHO)*, Oct. 2011, pp. 869–870, paper ThZ1.

Wangzhe Li (S'08) received the B.E. degree in electronic science and technology from Xi'an Jiaotong University, Xi'an, China, in 2004, and the M.Sc. degree in optoelectronics and electronic science from Tsinghua University, Beijing, China, in 2007. He is currently working toward the Ph.D. degree in electrical and computer engineering at the Microwave Photonics Research Laboratory, School of Electrical Engineering and Computer Science, University of Ottawa, Ottawa, ON, Canada.

His current research interests include photonic generation of microwave and terahertz signals.

Mr. Li is a recipient of a 2011 IEEE Microwave Theory and Techniques Society Graduate Fellowship and 2011 IEEE Photonics Society Graduate Fellowship.

Jianping Yao (M'99–SM'01–F'12) received the Ph.D. degree in electrical engineering from the Université de Toulon, France, in December 1997.

He joined the School of Electrical Engineering and Computer Science, University of Ottawa, ON, Canada, as an Assistant Professor in 2001. He was promoted to Associate Professor in 2003, and Full Professor in 2006. He was appointed University Research Chair in 2007. He was Director of the Ottawa-Carleton Institute for Electrical and Computer Engineering, from July 2007 to June 2010. Prior to joining the University of Ottawa, he was an Assistant Professor in the School of Electrical and Electronic Engineering, Nanyang Technological University, Singapore, from 1999 to 2011. His research has focused on microwave photonics, which includes photonic processing of microwave signals, photonic generation of microwave, mm-wave and THz, radio over fiber, UWB over fiber, and photonic generation of microwave arbitrary waveforms. His research also covers fiber optics and bio-photonics, which includes fiber lasers, fiber and waveguide Bragg gratings, fiber-optic sensors, microfluidics, optical coherence tomography, and Fourier-transform spectroscopy. He is a principal investigator of over 20 projects, including five strategic grant projects funded by the Natural Sciences and Engineering Research Council of Canada. He has published over 360 papers, including over 200 papers in peer-reviewed journals and 160 papers in conference proceedings.

Dr. Yao is an Associate Editor of the *International Journal of Microwave and Optical Technology*. He is on the Editorial Board of IEEE TRANSACTIONS ON MICROWAVE THEORY AND TECHNIQUES. He is a Chair of numerous international conferences, symposia and workshops, including Vice TPC Chair of 2007 IEEE Microwave Photonics Conference, TPC Co-Chair of 2009 and 2010 Asia-Pacific Microwave Photonics Conference, TPC Chair of the high-speed and broadband wireless technologies sub-committee of 2009, 2010, 2011, and 2012 IEEE Radio Wireless Symposium, TPC Chair of the microwave photonics sub-committee of 2009 IEEE Photonics Society Annual Meeting, TPC Chair of 2010 IEEE Microwave Photonics Conference, and General Co-Chair of 2011 IEEE Microwave Photonics Conference. He is also a committee member of numerous international conferences. He received the 2005 International Creative Research Award of the University of Ottawa. He was the recipient of the 2007 George S. Glinski Award for Excellence in Research. He was a recipient of a Natural Sciences and Engineering Research Council of Canada Discovery Accelerator Supplements award in 2008. Dr. Yao is a registered Professional Engineer of Ontario. He is a Fellow of the Optical Society of America, and a Fellow of the IEEE Microwave Theory and Techniques Society and the IEEE Photonics Society.